DOI: 10.1002/ejic.200701245

Platinum(II) Complexes with the Diethyl Aminomethylphosphonate Ligand (amp): Characterization, Properties, and Unusual Solution Behavior

Daniele Cornacchia,[a] Leonardo Cerasino,[a] Concetta Pacifico,[a] and Giovanni Natile*[a]

Keywords: Platinum / Diethyl aminomethylphosphonate / Antitumor agents / MMP inhibitors / Crystal structure

Cisplatin is one of the most widely prescribed drugs for the treatment of solid tumors, even though its pharmacological potential is often limited by side effects (nephrotoxicity, neurotoxicity, alopecia) and a limited spectrum of activity. Overcoming these limitations is one of the most chased goals by researchers in the field of medicinal chemistry. Since phosphonates have a great selectivity for bone tissues, we have extended a previous study on a platinum(II) complex with a diethyl [(methylsulfinyl)methyl]phosphonate (smp) ligand, [$PtCl_2$(*S,O*-smp)], to another phosphonate ester ligand, diethyl aminomethylphosphonate (amp). Further interest in this investigation was generated by the observation that [$PtCl_2$(*S,O*-smp)] was capable of inhibiting matrix metalloproteinases (MMPs), which also play a role in tumor growth. The interaction of the amp ligand with the tetrachloroplatinate(II) anion resulted in the production of the mono- and bis(amp) adducts in which the ligand acts as a monodentate *N*-coordinated species; however, no stable species with the chelating ligand could be isolated. A rationale for the different chelating abilities of amp and smp is offered. A solution of *cis*-[$PtCl_2$(*N*-amp)$_2$] in organic solvents is very stable if kept in the dark; if it is exposed to light, it undergoes a ready and clean *cis*/*trans* isomerization, affording the *trans*-[$PtCl_2$(*N*-amp)$_2$] complex. The compounds have been characterized by means of spectroscopic techniques (^{1}H, ^{31}P, and ^{195}Pt NMR), ESI-MS, and elemental analysis. In the case of *trans*-[$PtCl_2$(*N*-amp)$_2$], the X-ray structure has revealed a peculiar in-plane orientation of the amp ligand.

Introduction

Although Cisplatin (*cis*-ddp) is widely prescribed for the treatment of several solid tumors, such as testicular and ovarian carcinomas,[1] its pharmacological potential is limited by its side effects (in particular its toxicity to the kidneys) and the acquired or intrinsic resistance of many cancer types.[1,2] With the aim of overcoming these limitations, research has focused on the synthesis of new platinum complexes that could have better effectiveness and lower toxicity. In this context, platinum complexes with aminophosphonate ligands have been exploited as chemotherapeutic agents specific for the treatment of bone tumors.[3–7] Recently, it has also been found that platinum(II) complexes containing phosphonic acid ester ligands can act as inhibitors of matrix metalloproteinases (MMPs), a group of enzymes which plays a key role in the progress of metastasizing tumors. In particular, the complex [$PtCl_2$(*S,O*-smp)], in which smp stands for diethyl [(methylsulfinyl)methyl]phosphonate, was demonstrated to be an MMP inhibitor that is more effective than some inhibitors in clinical use.[8,9] This prompted us to extend the investigation to complexes with the diethyl aminomethylphosphonate ligand (amp, Scheme 1). In comparison to the smp ligand, amp has an amino group instead of a methylsulfinyl group. The amp ligand is virtually a bidentate ligand bearing two donor atoms: the nitrogen atom of the amine function and the nonalkylated oxygen atom of the phosphonate group. We succeeded in isolating monodentate *N*-coordinated amp complexes but failed in isolating any *N,O*-chelated species. We were aware of the fact that, contrary to (aminoalkyl)-phosphonates, which easily form *N,O*-chelates,[10] the corresponding diester species have only the P=O oxygen, a weak nucleophile, available for coordination to platinum. Nevertheless, we expected that amp would behave like smp,

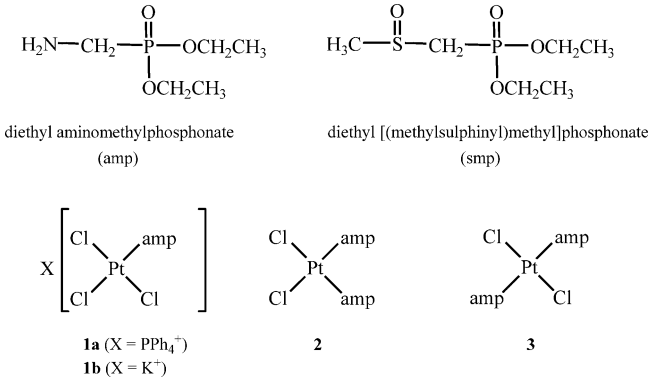

Scheme 1. Schematic view of the amp and smp ligands and of the complexes described in this paper.

[a] Università degli Studi di Bari, Dipartimento Farmaco-Chimico, via E. Orabona 4, 70125 Bari, Italy
Fax: +39-080-5442230
E-mail: natile@farmchim.uniba.it

which, although carrying a diethyl phosphonate moiety, is able to produce *S,O*-chelated species.

In this paper we describe the synthesis and characterization of three compounds, namely X[$PtCl_3$(*N*-amp)] [X = PPh_4^+ (**1a**) or K^+ (**1b**)], *cis*-[$PtCl_2$(*N*-amp)$_2$] (**2**), and *trans*-[$PtCl_2$(*N*-amp)$_2$] (**3**) (Scheme 1). Some peculiar features, such as a strong dependence of the $^3J_{Pt,P}$ upon the nature of the cation, the easy *cis*/*trans* isomerization of **2** to **3** if the sample is exposed to light, and the in-plane orientation of the amp ligand in the crystal structure of **3**, will be discussed. Moreover, a rationale for the different chelating abilities of amp and smp will be provided.

Results

Compound 1

Direct reaction between $(PPh_4)_2[PtCl_4]$ and amp 1:1 molar ratio in methanol/dichloromethane solution affords the monoadduct (PPh_4)[$PtCl_3$(*N*-amp)] (**1a**). The ^{1}H NMR spectrum of **1a** taken in $CDCl_3$ is shown in Figure 1a. The formation of the complex was confirmed by the shift of all ligand signals with respect to free amp (Table 1). The shift is particularly large for the central methylene proton signals (δ = 3.33 ppm; 0.24 ppm downfield), which, however, do not show resolved satellite peaks stemming from scalar coupling with platinum. The coupling with platinum is instead very well-resolved for the amino protons (δ = 3.66 ppm, $^2J_{H,Pt}$ = 52 Hz).

The amp phosphorus nucleus resonates at δ = 22.5 ppm (4.3 ppm upfield with respect to the free ligand) and has broad satellite peaks due to coupling with the metal center. The $^3J_{P,Pt}$ coupling constant is 220 Hz and falls in the range of values found for analogous compounds.[10] The phosphorus nucleus of the PPh_4^+ ion resonates at δ = 24.9 ppm (Figure 1b). In the ^{195}Pt NMR spectrum (Figure 1c), the platinum nucleus gives rise to a doublet (coupling with ^{31}P) centered at –1890 ppm. This chemical shift is consistent with a set of NCl_3 donor atoms, and falls in the range of values reported for a series of $[PtCl_3(NH_2–R)]^–$ compounds.[11]

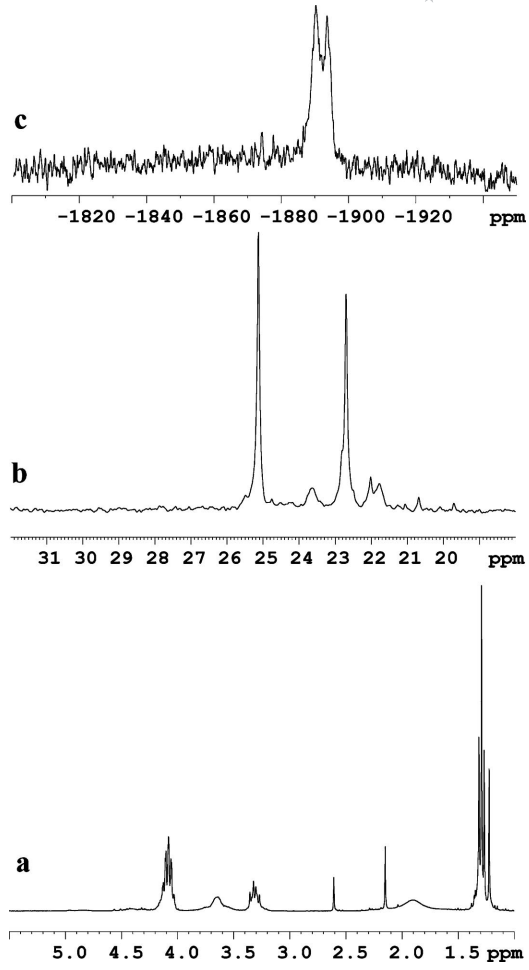

Figure 1. ^{1}H (a), ^{31}P (b), and ^{195}Pt NMR (c) spectra of compound **1a** in $CDCl_3$.

The ESI-MS spectrum of **1a** confirmed the given formula with a molecular peak at *m*/*z* = 467.6 corresponding to $[PtCl_3(amp)]^–$. The MS/MS spectrum of the parent ion shows only a major peak at *m*/*z* = 302.5 corresponding to $[M – amp]^–$.

Table 1. NMR spectroscopic data for the free amp ligand and related platinum complexes **1**–**3**. Chemical shifts are expressed in ppm: ^{1}H values are referenced to TSP in the case of D_2O and to residual solvent peaks in the case of other solvents; ^{31}P values are referenced to 85% H_3PO_4 (δ = 0 ppm); ^{195}Pt values are referenced to $PtCl_6^{2–}$ (δ = 0 ppm). Coupling constants are expressed in Hz.

Compd.	Solvent	NH_2	$^2J_{H,Pt}$	C–CH_2–O	$^3J_{H,P}$	N–CH_2–P	$^2J_{H,P}$/$^3J_{H,Pt}$	CH_3–C	^{31}P	$^3J_{P,Pt}$	^{195}Pt
amp	D_2O			4.16	7.3	3.08	10.9	1.32	30.9		
	$CDCl_3$	2.15		4.18	7.3	3.09	11.0	1.33	26.9		
	[D_6]acetone	N.A.		4.09	7.9	3.23	17.2	1.26	23.8		
1a	$CDCl_3$	3.66	52	4.10	8.3	3.33	10.1/[a]	1.31	22.7[b]	220	–1890
	[D_6]acetone	3.92	[c]	4.11	8.5	3.19	10.9/[a]	1.29	22.5[d]	216	[e]
1b	D_2O			4.29	8.1	3.32	12.4/27	1.40	24.5	161	–1925
	[D_6]acetone	4.23	[c]	4.17	8.4	3.26	11.4/[a]	1.31	22.8	194	[e]
2	D_2O			4.30	7.9	3.38	11.9/26	1.42	25.1	166	–2220
	$CDCl_3$	5.12	57	4.31	7.7	3.34	13.2/34	1.43	24.8	76	[e]
3	D_2O			4.24	8.1	3.24	12.4/20	1.36	24.9	140	–2198
	$CDCl_3$	3.88	54	4.19	8.4	3.25	11.0/[a]	1.38	21.3	200	[e]

[a] Not determined because satellites overlap with the main peak. [b] The PPh_4^+ phosphorus nucleus resonates at δ = 25.2 ppm. [c] Not determined because the signal is very broad. [d] The PPh_4^+ phosphorus nucleus resonates at δ = 24.7 ppm. [e] Data not available.

Performing an analogous reaction between $K_2[PtCl_4]$ and amp in water solution, the same monoadduct can be isolated as potassium salt **1b**. The NMR spectra of **1b** were substantially identical to those of **1a** and will not be commented on in detail. It is, however, worth mentioning a significantly smaller coupling constant between platinum and phosphorus (161 instead of 220 Hz) and a broad peak for platinum with unresolved coupling with the phosphorus nucleus.

Compound 2

The bis adduct *cis*-$[PtCl_2(N\text{-amp})_2]$ can be obtained in good yield by the reaction of $K_2[PtCl_4]$ and amp (1:2 molar ratio) in water solution. The ^{1}H NMR spectrum of **2** in $CDCl_3$ is shown in Figure 2a. Complex formation was confirmed by the change in the chemical shift of all ligand signals with respect to free amp. The central methylene protons give a multiplet (δ = 3.34 ppm), which is shifted 0.25 ppm downfield with respect to the free ligand. The downfield shift is 0.13 and 0.09 ppm for the ethoxy methylene and methyl protons, respectively. The amino protons give a broad doublet due to coupling with the phosphorus nucleus (with a coupling constant of 17.4 Hz). This multiplicity disappears in the ^{31}P-decoupled ^{1}H NMR spectrum, where a broad singlet with satellite peaks due to coupling with the platinum nucleus ($^2J_{H,Pt}$ = 57 Hz) is observed. The central methylene protons give a doublet of triplets (δ = 3.34 ppm) as a result of ^2J coupling with the phosphorus nucleus (13.17 Hz) and ^3J coupling with the two amino protons (ca. 6.6 Hz). The ^{31}P NMR spectrum (Figure 2b) shows a singlet at δ = 24.8 ppm (1.07 ppm upfield with respect to the free ligand) with broad satellite peaks due to coupling with platinum ($^3J_{P,Pt}$ = 76 Hz). This value of $^3J_{P,Pt}$ is considerably smaller than the values found for compounds **1** and **3** in $CDCl_3$ (220 and 200 Hz, respectively). However, the $^3J_{P,Pt}$ value is larger in D_2O (166 Hz) and comparable to those found for **1** and **3** in the same solvent (161 and 140 Hz, respectively).

In the ^{195}Pt spectrum (Figure 2c), a broad signal is visible at –2220 ppm. Such a broadening with respect to the corresponding signal in compound **1** is due to the increased number of *N*-donor ligands and the unresolved coupling with ^{31}P. The value of the chemical shift is compatible with a set of N_2Cl_2 donor atoms.

The formula of the compound was confirmed by the ESI-MS spectrum (parent peak at *m*/*z* = 622.7 corresponding to $[\{PtCl_2(amp)_2\} + Na]^+$) and the MS/MS spectrum of the parent ion (major fragments at *m*/*z* = 455.8 [M – amp + Na]$^+$ and 419.8 [M – amp – HCl + Na]$^+$).

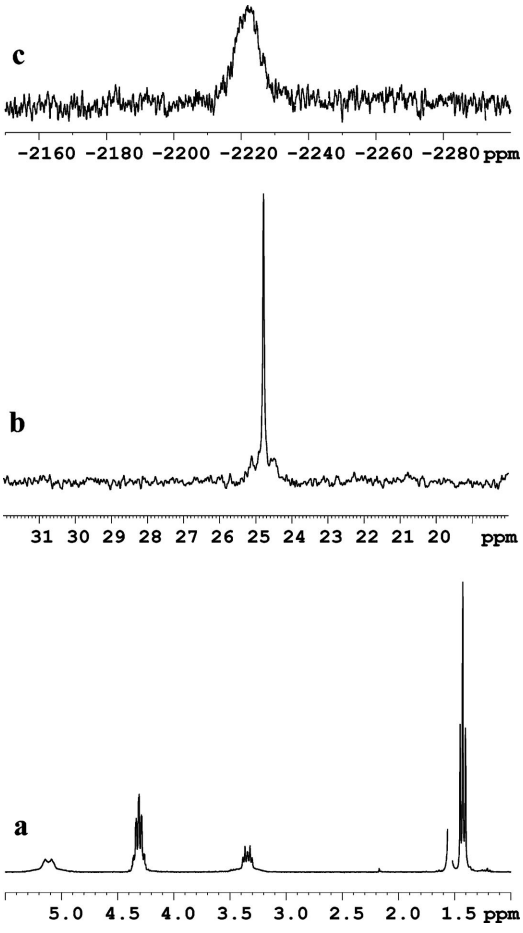

Figure 2. ^{1}H (a), ^{31}P (b), and ^{195}Pt NMR (c) spectra of compound **2** in $CDCl_3$.

Compound 3

Compound **2** dissolved in dichloromethane and layered under diethyl ether, if not kept in the dark, undergoes *cis*/*trans* isomerization to afford yellow crystals of *trans*-$[PtCl_2(N\text{-amp})_2]$ (**3**). The ^{1}H NMR spectrum of **3** in $CDCl_3$ is shown in Figure 3a. As in the previous cases, complex formation has been confirmed by the downfield shift of all proton signals with respect to the free ligand. The changes in chemical shifts are 0.16, 0.01, and 0.05 ppm downfield for the central methylene, the ethoxy methylene and methyl protons, respectively. Moreover, the amino protons have satellite peaks due to coupling with the platinum atom ($^2J_{H,Pt}$ = 54 Hz). In the ^{31}P NMR spectrum (Figure 3b), a unique signal is visible at δ = 21.3 ppm (5.6 ppm upfield with respect to the free ligand). The signal has broad satellites due to coupling with the platinum nucleus, with a $^3J_{P,Pt}$ coupling constant of 200 Hz.

In the ^{195}Pt spectrum (Figure 3c), the species exhibits a broad signal at –2198 ppm with unresolved coupling with the phosphorus nucleus. The value of the chemical shift is compatible with a set of N_2Cl_2 donor atoms and is comparable to that found for **2**.

In the ESI-MS spectrum, the parent ion is at *m*/*z* = 622.9 $\{[PtCl_2(amp)_2] + Na\}^+$, and the MS/MS spectrum of the parent ion has major fragments at *m*/*z* = 455.9 [*M* – amp + Na]$^+$ and *m*/*z* = 419.9 [*M* – amp – HCl + Na]$^+$.

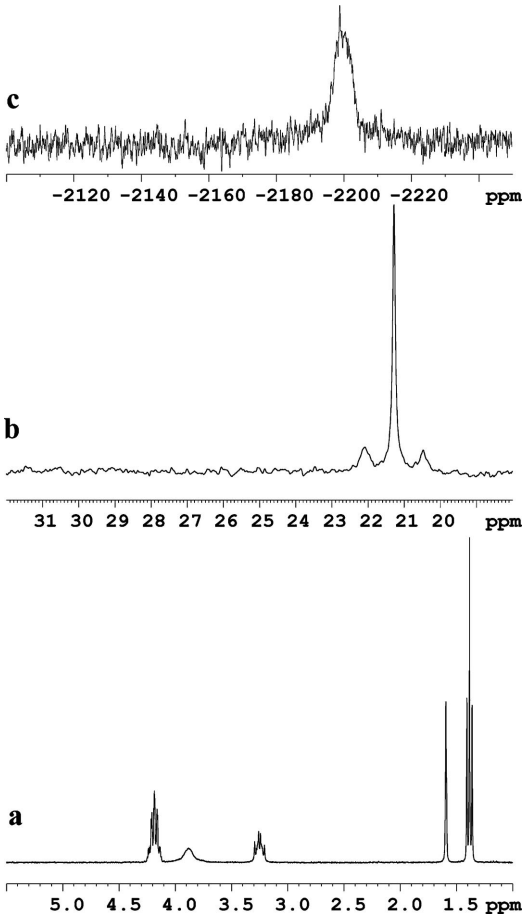

Figure 3. ^{1}H (a), ^{31}P (b), and ^{195}Pt NMR (c) spectra of compound **3** in $CDCl_3$.

X-ray Diffraction Analysis of 3

Yellow crystals of *trans*-[$PtCl_2$(*N*-amp)$_2$] were obtained by crystallization of the *cis* isomer **2** from a mixture of dichloromethane and diethyl ether (1:1, v/v). The asymmetric unit comprises one independent molecule of the substrate. An ORTEP drawing of **3** is shown in Figure 4. A selection of bond lengths and angles is listed in Table 2.

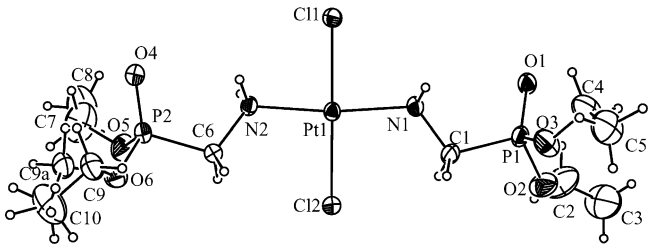

Figure 4. A view of the asymmetric unit of *trans*-[$PtCl_2$(*N*-amp)$_2$], showing the atomic numbering scheme. Displacement ellipsoids are drawn at the 30% probability level.

The platinum center has a square-planar coordination. The deviations [Å] from the least-squares plane defined by the four donor atoms are: Pt –0.0075(3), Cl1 0.002(2), Cl2 0.003(2), N1 –0.016(5), and N2 –0.014(5). The Pt–N–C–P torsion angles are 174.8(3)° and 171.0(3)° for the two amp ligands, in accord with a *transoid* disposition which brings the bulky platinum and phosphorus-centered moieties farther away. Moreover, the phospohonate group is rotated in such a way as to direct the P=O oxygen atom (electron-rich) towards the amine protons (electron-deficient), forming an intraligand hydrogen bond [N1···O1 3.00(1) Å, (N1)H11···O1 2.60(1) Å, N1–H11···O1 108(1)°; N2···O4 3.00(1) Å, (N2)H21···O4 2.56(1) Å, N2–H21···O4 110(1)°]. The N–C–P=O torsion angles for the two amp ligands are 25.2(6)° and 24.4(6)°. It is surprising that the dihedral angles between the platinum coordination plane and the ligand planes (through the atoms N–C–P) are very small (3° and 11°). In square-planar complexes the ligand planes usually tend to be orthogonal to the coordination plane in order to minimize steric interactions between *cis* ligands. A possible explanation for this unusual conformation is that the in-plane orientation of each amp ligand is fostered by favorable electrostatic interactions between the amine protons and the *cis* chlorido ligand [average N···Cl and (N)H···Cl distances of 3.00 and 2.93 Å, respectively], and between the protons of the methylene group bridging the N and P atoms of the amp ligands and the second chlorido ligand [average C···Cl and (C)H···Cl distances of 3.20 and 2.95 Å, respectively]. In several occasions, theoretical investigations[12] have suggested the existence of positive electrostatic interactions between amino and *cis* chlorido ligands. The occurrence of such an interaction also in the present case is fully supported by the narrowing of the two Cl–Pt–N angles (average 86.3°) where the amine protons reside. In the complex, one ethyl group (C9/C9a) is disordered.

Table 2. Selected bond lengths [Å] and angles [°] for **3**.

Bond lenghts		Angles	
Pt1–N2	2.064(5)	N2–Pt1–N1	172.7(2)
Pt1–N1	2.064(5)	N2–Pt1–Cl2	93.5(2)
Pt1–Cl2	2.304(2)	N1–Pt1–Cl2	93.8(2)
Pt1–Cl1	2.309(2)	N2–Pt1–Cl1	86.3 (2)
N1–C1	1.457(8)	N1–Pt1–Cl1	86.4(2)
N2–C6	1.474(8)	Cl2–Pt1–Cl1	179.5(1)
C1–P1	1.801(7)	C1–N1–Pt1	123.2(4)
P1–O1	1.460(5)	C6–N2–Pt1	122.6(4)
P1–O2	1.560(7)	N1–C1–P1	112.7(5)
P1–O3	1.562(6)	N2–C6–P2	111.6(4)
P2–O4	1.466(5)		
P2–O6	1.561(5)		
P2–O5	1.567(6)		

Crystal Packing

Molecules are piled along the *a* direction (Figure 5). Adjacent molecules are displaced in such a way as to align the chlorido ligand of one molecule with the platinum atoms of the two sandwiching molecules, the Pt···Cl distance being 4.02 Å. Each molecule of the pile donates hydrogen bonds (N–H···O=P) to the two adjacent molecules [N1···O4(2 – *x*, –*y*, 1 – *z*) 2.98(1) Å, (N1)H12···O4(2 – *x*, –*y*, 1 – *z*) 2.08(1) Å, N1–H12···O4(2 – *x*, –*y*, 1 – *z*) 177(1)°, N2···O1(1 – *x*, –*y*, 1 – *z*) 2.95(1) Å, (N2)H22···O1(1 – *x*, –*y*,

1 – *z*) 2.05(1) Å, N2–H22···O1(1 – *x*, –*y*, 1 – *z*) 172(1)°] while accepting symmetrically related hydrogen bonds from them.

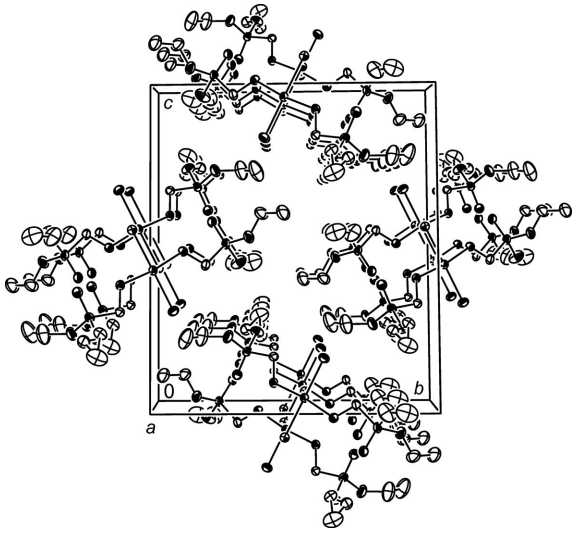

Figure 5. View of the crystal packing along the *a* axis of *trans*-[$PtCl_2$(*N*-amp)$_2$].

Within the pile of molecules running along the *a* direction the Pt–Cl bonds are nearly orthogonal to the *a* direction (92.7°) while the Pt–N bonds are slanted to the *a* direction (57.2°). The result is that the distances between the planes defined by the four donor atoms of two adjacent molecules [alternatively 3.409(1) and 3.413(1) Å] are shorter than the distance between Pt···Cl atoms aligned in the *a* direction (4.02 Å).

Complex chains extending along the *a* direction are held together by weak hydrogen bonds between ethyl protons of the phosphonate groups and the chlorido ligands.

Discussion and Conclusions

There are some features of the compounds just described which deserve further discussion. In particular: (i) the spontaneous isomerization of *cis*-[$PtCl_2$(*N*-amp)$_2$] (**2**) to *trans*-[$PtCl_2$(*N*-amp)$_2$] (**3**), (ii) the great variation of $^3J_{P,Pt}$ as a function of the solvent as observed for compound **2**, and (iii) the instability of the *N*,*O*-chelate form of the amp ligand.

Study of the *cis*/*trans* Isomerization of *cis*-[$PtCl_2$(*N*-amp)$_2$] (2)

As described in detail in the Experimental Section, when *cis*-[$PtCl_2$(*N*-amp)$_2$] (**2**) is dissolved in a mixture of CH_2Cl_2 and diethyl ether (1:1, v/v) and kept in a vial, it undergoes isomerization, and nice crystals of the corresponding *trans* isomer **3** form in two days. It took us some time to realize that the isomerization was purely photochemical and can be completely prevented if the sample is kept in the dark.

In general, the *cis*/*trans* isomerization of square-planar complexes can occur by two major mechanisms: the dissociative mechanism and the associative mechanism (Scheme 2).[13a–13g] In the dissociative path,[13a–13e] the initial square-planar complex (let us assume it has *cis* configuration) loses one ligand to form a T-shaped intermediate/transition state (often stabilized by loose association of a solvent molecule), which can easily isomerize to a second T-shaped intermediate/transition state in which the two formerly *cis* ligands are now *trans*. Reassociation of the ligand dissociated in the first step would afford the *trans* complex. The dissociative mechanism generally requires the presence of a strong *trans*-labilizing ligand or of particularly bulky ligands that can relieve the strain in the coordination shell by the dissociation of one donor group.[14] In the associative mechanism,[13f–13g] the presence of a catalytic amount of a free ligand and the occurrence of two consecutive ligand substitution processes are necessary. Starting with a *cis*-[MX_2A_2] complex and a catalytic amount of A, the first ligand substitution (replacement of X by A) leads to [MXA_3], and the second substitution process (reentering of the displaced X into the complex and loss of one A) leads to *trans*-[MX_2A_2]. Generally, the rate of isomerization is subject to variation with temperature regardless of whether the mechanism is associative or dissociative.

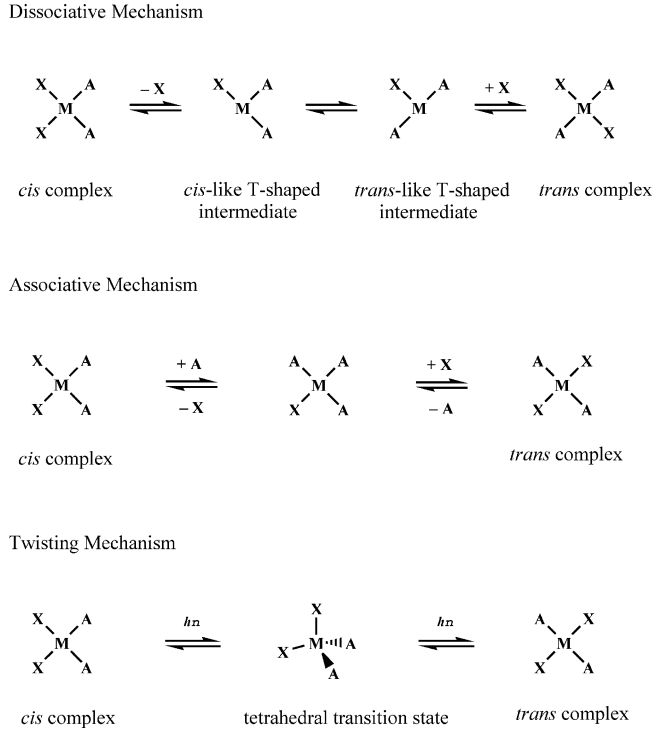

Scheme 2. Schematic view of the three possible *cis*/*trans* isomerization mechanisms.

A third mechanism can be hypothesized in which the isomerization takes place without bond-breaking and bond-making; however, this mechanism requires passing from a square-planar to a tetrahedral structure and vice-versa. Although this mechanism results to be symmetry-forbidden, photochemical isomerization of square-planar metal com-

plexes by such a mechanism has already been reported.[15] The photochemical isomerization mechanism is also represented in Scheme 2.

The observation of isomerization only in the presence of light led us to conclude that in the present case the isomerization process occurs by photoactivation and involves a tetrahedral transition state without bond dissociation.

Variability of $^3J_{P,Pt}$ in Compound 2

Another observation which deserves an explanation is why the $^3J_{P,Pt}$ coupling, usually in the range 160–210 Hz (compounds **1** and **3**), was as small as 70 Hz for compound **2** in $CDCl_3$ solution. In general, the ^3J coupling constant is deeply affected by the value of the three-bond (Pt–N–C–P) torsion angle according to the Karplus rule:[16] a greater coupling constant is expected for a torsion angle close to zero (this would be the case for a *N*,*O*-chelated amp ligand) or to 180° (as in the case of the monodentate amp ligand observed in the crystal structure of **3**). For some reason, for compound **2** in $CDCl_3$ solution, the Pt–N–C–P torsion angle is intermediate between 0 and 180°, so as to justify a $^3J_{P,Pt}$ that is about one third the usual value. This could be a consequence of specific interactions between monodentate *cis*-coordinated amp ligands. We wanted to check if this interligand interaction between *cis* amp ligands could be disrupted by changing the ionic strength of the medium. As matter of fact, addition of an equimolar amount of $(PPh_4)Cl$ brings the $^3J_{P,Pt}$ coupling constant in $CDCl_3$ solution to the usual value of ca. 200 Hz.

A Rationale for the Instability of the Chelated Form of the amp Ligand

Another feature of the amp ligand is the instability of the *N*,*O*-chelated form. We were aware of the fact that, relative to aminomethylphosphates, dialkyl aminomethylphosphonates are less susceptible to undergo chelation, since the only phosphorus-bound oxygen still available for coordination to platinum has sp^2 hybridization and does not carry negative charge. However, the preparation of the *S*,*O*-chelated form of the closely related diethyl [(methylsulfinyl)-methyl]phosphonate species was rather promising. The most straightforward procedure for obtaining the *N*,*O*-chelated form that we could think of was treatment of trichlorido species **1** with silver nitrate. The reaction, performed in water, leads to the formation of a new species characterized by a slight upfield shift of the signals due to central methylene protons (δ = 3.18 ppm; 0.14 ppm upfield with respect to **1**) and to the phosphorus nucleus (δ = 23.8 ppm; 0.7 ppm upfield with respect to **1**). The ESI-MS spectrum of the final solution showed a molecular peak at *m*/*z* = 494.6, corresponding to $\{[PtCl_2(amp)] + NO_3\}^-$ in the negative current and two peaks at *m*/*z* = 455.8 and 471.8, corresponding to $\{[PtCl_2(amp)] + Na\}^+$ and $\{[PtCl_2(amp)_2] + K\}^+$, respectively, in the positive current. However, other species were also present in the solution, and any attempt to isolate the pure $[PtCl_2(amp)]$ compound was unsuccessful. The *N*,*O*-chelated species was clearly unstable and formed several by-products, thus indicating that amp does not stabilize chelation as much as smp. We can provide a rationale for this difference in behavior. We have to consider specific properties that could favor smp chelation and disfavor amp chelation. Chelation of smp could be promoted by two factors. One factor is the presence of two bulky substituents on the sulfur atom (the $-CH_3$ and the O atom as compared to the two protons present on the nitrogen atom of amp). Steric repulsion between the substituents on sulfur and those on phosphorus (the two ethoxy groups) can favor a gauche disposition of the *S*- and (P)*O*-donor atoms and favor the chelation of smp to platinum. The gauche conformation of the smp ligand found in the X-ray structure of $K[PtCl_3(smp)]$ with monodentate *S*-bound smp (Pt–S–C–P torsion angle of 58°) lends support to this conclusion.[17] This effect is similar to that first described by Thorpe and Ingold in relation to the cyclization of organic moieties[18a–18c] and discussed in greater detail in later work.[19] An additional factor that could favor chelation of smp is the *cis*-labilizing effect of the coordinated sulfoxide group,[20a–20d] which could favor the release of a *cis*-chlorido ligand in the adduct with monocoordinated smp. Once the chelate ring has been formed, the sulfur-bound oxygen points outward from the chelate ring and does not labilize the *cis*-coordinated phosphonic group. We can also consider features of the amp ligand which could prevent the coordination of the P=O oxygen to platinum. The X-ray structure of compound **3** has shown that monodentate amp has a *transoid* conformation with a Pt–N–C–P torsion angle of 172°. Such a conformation, while favoring intraligand N–H···O=P hydrogen bond formation, certainly disfavors the coordination of the P=O oxygen atom to platinum.

As a final comment, we want to recall that the aim of this study was the preparation of compounds that could possibly have an inhibitory effect on MMP. We believe that the best candidate for this investigation is compound **1**, which will shortly undergo a complete series of biological tests.

Experimental Section

Starting Compounds: $(PPh_4)_2[PtCl_4]$ was prepared from $K_2[PtCl_4]$ by using the procedure reported in the literature for the preparation of $(AsPh_4)_2[PtCl_4]$,[21] and ampH hydrogen oxalate was purchased from Acros Organics, Belgium.

Preparation of the Complexes: The free amp ligand was obtained from the commercial hydrogen oxalate salt by treatment with a base. Briefly, a water solution of the ampH hydrogen oxalate was treated with a stoichiometric amount of calcium oxide, and the insoluble calcium oxalate was removed by filtration of the water solution. The aminomethylphosphonate could be recovered from the aqueous solution by evaporation of the solvent under reduced pressure.

$(PPh_4)[PtCl_3(N\text{-amp})]$ (1a): $(PPh_4)_2[PtCl_4]$ (264.0 mg, 0.26 mmol), dissolved in a mixture of methanol (5 mL) and dichloromethane (7 mL), was treated with amp (0.26 mmol dissolved in 2 mL meth-

anol). The mixture was stirred at room temperature for 2 h. The resulting brown solution was concentrated to dryness by evaporation of the solvents under reduced pressure. The resulting brown solid was treated with methanol (10 mL), the yellow solution was filtered (to remove a dark-gray residue of PPh_4Cl mixed with metallic platinum) and concentrated to dryness by evaporation of the solvent under reduced pressure. The yellow residue was demonstrated to be a mixture of compound **1a**, PPh_4Cl, unreacted $(PPh_4)_2[PtCl_4]$, and other byproducts. Chromatographic purification on a silica gel column, by using dichloromethane/acetone (1:1) as eluant, afforded pure compound **1a** (48.0 mg, 23% yield). The compound was characterized by IR, ^1H, ^{31}P and ^{195}Pt NMR spectroscopy, ESI-MS, and elemental analysis. $C_{29}H_{34}Cl_3NO_3P_2Pt$ (807.75): calcd. C 43.12, H 4.21, N 1.73; found C 42.90, H 4.35, N 1.65. ESI-MS: m/z = 467.6 $[Pt(amp)Cl_3]^-$ (in the negative current), 339 $[PPh_4]^+$ (in the positive current).

K[PtCl$_3$(*N*-amp)] (1b): A solution of amp (0.72 mmol) in water (2.5 mL) was added dropwise, at room temperature, to a solution of $K_2[PtCl_4]$ (300.0 mg, 0.72 mmol) in the same solvent (1.0 mL). The red solution was stirred for 24 h. During this time, a drift to lower pH was observed, which required additions of small aliquots of KOH (3.5 M) in order to keep the pH close to 7. The aqueous solution was treated with dichloromethane in order to remove traces of the neutral bis adduct *cis*-$[PtCl_2(N\text{-amp})_2]$ (compound **2**), which is soluble in the chlorinated solvent. The organic phase was removed, and the aqueous phase was concentrated to dryness by evaporation of the solvent under reduced pressure. The solid residue was treated with absolute ethanol, the solution was filtered to remove insoluble KCl and $K_2[PtCl_4]$ and then treated with diethyl ether, which induced the formation of an orange precipitate (very hygroscopic) of compound **1b** (179.2 mg, 49% yield). The compound was characterized by IR, ^1H, ^{31}P and ^{195}Pt NMR spectroscopy, ESI-MS, and elemental analysis. $C_5H_{14}Cl_3KNO_3PPt$ (507.61): calcd. C 11.83, H 2.76, N 2.76; found C 12.03, H 2.80, N 2.73. ESI-MS: m/z = 467.6 $[Pt(amp)Cl_3]^-$ (in the negative current).

***cis*-[PtCl$_2$(*N*-amp)$_2$] (2):** A solution of amp (0.96 mmol) in water (2 mL) was added dropwise, at room temperature, to a solution of $K_2[PtCl_4]$ (200.0 mg, 0.48 mmol) in water (1 mL). The red solution was stirred for 48 h under argon. During this time, a drift to lower pH was observed, which required additions of small aliquots of KOH (3.5 M) in order to keep the solution neutral. Extraction with dichloromethane (3 × 50 mL) afforded an organic fraction, which was concentrated to dryness under reduced pressure. After trituration of the oily residue with diethyl ether, compound **2** was obtained as a yellow solid (141.6 mg, 49% yield). The compound was characterized by IR, ^1H, ^{31}P and ^{195}Pt NMR spectroscopy, ESI-MS, and elemental analysis. $C_{10}H_{28}Cl_2N_2O_6P_2Pt$ (600.12): calcd. C 20.01, H 4.70, N 4.67; found C 20.13, H 4.68, N 4.62. ESI-MS: m/z = 623 $[M + Na]^+$.

***trans*-[PtCl$_2$(*N*-amp)$_2$] (3):** A solution of **2** (80.0 mg, 0.13 mmol) in a 1:1 (v/v) mixture (3 mL) of dichloromethane and diethyl ether was kept under unfiltered light at room temperature. Pale yellow needles of **3** separated out in 48 h. They were collected, washed with cold dichloromethane, and dried in vacuo. The compound was characterized by IR, ^1H, ^{31}P and ^{195}Pt NMR spectroscopy, ESI-MS, and elemental analysis. $C_{10}H_{28}Cl_2N_2O_6P_2Pt$ (600.12): calcd. C 20.01, H 4.70, N 4.67; found C 20.66, H 4.75, N 4.77. ESI-MS: m/z = 623 $[M + Na]^+$.

Physical Measurements: NMR spectra were collected at 298 K with a Bruker DPX 300 MHz spectrometer. Monodimensional ^{31}P and ^{195}Pt spectra were acquired by using ^1H-decoupling sequences. FTIR spectra were recorded with a Perkin–Elmer mod. 283 Spectrum One System. Elemental analysis were carried out with a CHN Eurovector EA 3011 instrument. ESI-MS analysis was performed with an Agilent 1100 series LC-MSD Trap system VL.

X-ray Diffraction Analysis: X-ray data were collected with a Bruker AXS X8 APEX CCD system equipped with a four-circle Kappa goniometer and a 4 K CCD detector (radiation Mo-K_α). A total of 50687 reflections (Θ_{max} = 30, 45°) were indexed, integrated, and corrected for Lorentz, polarization, and absorption effects by using multi-scan. 6610 were independent reflections. The unit cell dimensions were calculated from all reflections. The structure was solved by direct methods in the $P2_1/c$ space group. The model was refined by full-matrix least-squares methods. Anisotropic thermal parameters were applied for all non-hydrogen atoms. The hydrogen atoms were located and refined isotropically. The weighting scheme employed was $w = 1/[\sigma^2(F_o^2) + (0.0286P)^2 + 6.6000P]$ where $P = (F_o^2 + 2F_c^2)/3$. The refinement converged to R_1 = 0.0410, wR_2 = 0.0773, and S = 1.066 for 4157 reflections with $I > 2\sigma(I)$, and R_1 = 0.0896, wR_2 = 0.0972, and S = 1.066 for 6610 unique reflections and 222 parameters. The final difference Fourier map showed electron density peaks (up to 1.0 e Å^{-3}) lying near the Pt atoms. All calculations were performed and molecular graphics were drawn by using the SIR2002,[22] SHELXL-97,[23] PARST97,[24,25] WinGX,[26] and ORTEP-3 for Windows packages.[27] The crystallographic data are listed in Table 3.

Table 3. Experimental details for the crystallographic analysis of **3**.

Empirical formula	$C_{10}H_{28}Cl_2N_2O_6P_2Pt$
Formula weight	600.27
Temperature	293(2) K
Wavelength	0.71073 Å
Crystal system, space group	monoclinic, $P2_1/c$
Unit cell dimensions	a = 8.0966(2) Å
	b = 15.3135(5) Å
	c = 17.7484(6) Å
	α = 90°
	β = 98.788(2)°
	γ = 90°
Volume	2174.74(12) Å^3
Z	4
Calculated density	1.833 Mg m^{-3}
Absorption coefficient	6.868 mm^{-1}
F(000)	1168
Crystal size	0.1 × 0.11 × 2.51 mm
Θ range for data collection	1.77–30.45°
Limiting indices	$-11 \le h \le 11$, $-21 \le k \le 21$, $-25 \le l \le 25$
Reflections collected/unique	50687/6610 [R(int) = 0.0709]
Completeness to Θ = 30.45	100.0%
Refinement method	Full-matrix least-squares on F^2
Data/restraints/parameters	6610/6/222
Goodness-of-fit on F^2	1.066
Final R indices [$I > 2\sigma(I)$]	$R1$ = 0.0410, $wR2$ = 0.0773
R indices (all data)	$R1$ = 0.0896, $wR2$ = 0.0972
Extinction coefficient	0.00064(9)
Largest diff. peak and hole	1.294 and –0.846 e Å^{-3}

CCDC-673719 contains the supplementary crystallographic data for this paper. These data can be obtained free of charge from The Cambridge Crystallographic Data Centre via www.ccdc.cam.ac.uk/data_request/cif.

Acknowledgments

This research was supported by the University of Bari, the Italian "Ministero dell'Universitá e della Ricerca (MUR)" (PRIN 2004 no. 20040590-78) and the EC (COST D39).

[1] P. O'Dwyer, J. Stevenson, S. Johnson, "Clinical Status of Cisplatin, Carboplatin and Other Platinum-Based Antitumor Drugs" in *Cisplatin: Chemistry and Biochemistry of a Leading Anticancer Drug* (Ed.: B. Lippert), Verlag Helvetica Chimica Acta, Zurich, **1999**.

[2] D. D. Von Hoff, R. Schilsky, C. M. Reichert, R. L. Reddick, M. Rozencweig, R. C. Young, F. M. Muggia, *Cancer Treat. Rep.* **1979**, *63*, 1527–1531.

[3] T. Klenner, P. Valenzuela-Paz, B. K. Keppler, G. D. Augres, H. R. Scherf, F. Wingen, D. Schmähl, *Cancer Treat. Rev.* **1990**, *17*, 253–259.

[4] T. Klenner, P. Valenzuela-Paz, F. Amelung, H. Munch, H. Zahn, B. K. Keppler, H. Blum in *Metal Complexes in Cancer Chemotherapy* (Ed.: B. K. Keppler), VCH, Weinheim, **1993**, pp. 85–127.

[5] F. Wingen, D. Scmahl, *Arzneim.-Forsch./Drug Res.* **1985**, *35*, 1565–1571.

[6] J. H. Lin, *Bone* **1996**, *18*, 75–85.

[7] B. K. Keppler, M. R. Berger, T. Klenner, M. E. Heim, *Adv. Drug Res.* **1990**, *19*, 243–310.

[8] M. Laforgia, L. Cerasino, N. Margiotta, M. A. M. Capozzi, C. Cardellicchio, F. Naso, G. Natile, *Eur. J. Inorg. Chem.* **2004**, 3445–3452.

[9] R. Sasanelli, A. Boccarelli, D. Giordano, M. Laforgia, F. Arnesano, G. Natile, C. Cardellicchio, M. A. M. Capozzi, M. Coluccia, *J. Med. Chem.* **2007**, *50*, 3434–3441.

[10] T. G. Appleton, J. R. Hall, I. J. McMahon, *Inorg. Chem.* **1986**, *25*, 720–725.

[11] P. S. Pregosin, *Coord. Chem. Rev.* **1982**, *44*, 247–291.

[12] P. Carloni, W. Andreoni, J. Hutter, A. Curioni, P. Giannozzi, M. Parrinello, *Chem. Phys. Lett.* **1995**, *234*, 50–56.

[13] a) R. Romeo, L. Monsù Scolaro, N. Nastasi, B. E. Mann, G. Bruno, F. Nicolò, *Inorg. Chem.* **1996**, *35*, 7691–7698; b) R. Romeo, G. Alibrandi, *Inorg. Chem.* **1997**, *36*, 4822–4830; c) W. J. Louw, R. van Eldik, *Inorg. Chem.* **1981**, *20*, 1939–1941; d) R. Romeo, D. Minniti, M. Trozzi, *Inorg. Chim. Acta* **1975**, *14*, L15–L16; e) R. Romeo, D. Minniti, M. Trozzi, *Inorg. Chem.* **1976**, *15*, 1134–1138; f) W. J. Louw, *Inorg. Chem.* **1977**, *16*, 2147–2160; g) R. Roulet, C. Barbey, *Helv. Chim. Acta* **1973**, *56*, 2179–2186.

[14] a) R. Romeo, D. Minniti, S. Lanza, *Inorg. Chem.* **1980**, *19*, 3663–3668; b) F. P. Fanizzi, M. Lanfranchi, G. Natile, A. Tiripicchio, *Inorg. Chem.* **1994**, *33*, 3331–3339; c) F. P. Fanizzi, N. Margiotta, M. Lanfranchi, A. Tiripicchio, G. Pacchioni, G. Natile, *Eur. J. Inorg. Chem.* **2004**, 1705–1713.

[15] a) M. O. Santiago, C. L. Donicci Filho, I. Moreira, R. M. Carlos, S. L. Queiroz, A. A. Batista, *Polyhedron* **2003**, *22*, 3205–3211; b) S. H. Mastin, P. Haake, *J. Chem. Soc., D* **1970**, 202.

[16] M. Karplus, *J. Am. Chem. Soc.* **1963**, *85*, 2870–2871.

[17] M. Laforgia, N. Margiotta, F. Capitelli, V. Bertolasi, G. Natile, *Eur. J. Inorg. Chem.* **2005**, 1710–1715.

[18] a) R. M. Beesley, C. K. Ingold, J. F. J. Thorpe, *J. Chem. Soc.* **1915**, 1080–1106; b) C. K. Ingold, *J. Chem. Soc.* **1921**, 305–329; c) S. W. Smith, M. S. Newman, *J. Am. Chem. Soc.* **1968**, *90*, 1253–1257.

[19] M. E. Jung, J. Gervay, *J. Am. Chem. Soc.* **1991**, *113*, 224–232.

[20] a) P. Kapoor, K. Lövqvist, Å. Oskarsson, *J. Mol. Struct.* **1998**, *470*, 39–47; b) Z. Bugarcic, K. Lövqvist, Å. Oskarsson, *Acta Chem. Scand.* **1993**, *47*, 554–559; c) V. Y. Kukushkin, V. K. Belsky, G. A. Kirakosyan, L. V. Kanovalov, A. I. Moiseev, V. M. Tkachuk, *Inorg. Chim. Acta* **1991**, *185*, 143–154; d) P. D. Braddock, R. Romeo, M. L. Tobe, *Inorg. Chem.* **1974**, *13*, 1170–1174.

[21] R. Z. Pellicani, F. P. Intini, L. Maresca, E. Mesto, C. Pacifico, G. Natile, *Eur. J. Inorg. Chem.* **2006**, 1635–1642.

[22] M. C. Burla, M. Camalli, B. Carrozzini, G. L. Cascarano, C. Giacovazzo, G. Polidori, R. Spagna, *J. Appl. Crystallogr.* **2003**, *36*, 1103.

[23] G. M. Sheldrick, *SHELXL-97, Programs for Crystal Structure Analysis (Release 97–2)*, University of Göttingen, Germany, **1998**.

[24] M. Nardelli, *Comput. Chem.* **1983**, *7*, 95–97.

[25] M. Nardelli, *J. Appl. Crystallogr.* **1995**, *28*, 659.

[26] L. J. Farrugia, *J. Appl. Crystallogr.* **1999**, *32*, 837–838.

[27] L. J. Farrugia, *J. Appl. Crystallogr.* **1997**, *30*, 565.

Received: November 20, 2007
Published Online: February 22, 2008

